J. Fluid Mech. (2007), *vol.* 588, *pp.* 309–330.
doi:10.1017/S0022112007007744 Printed in the United Kingdom

The trailing-edge problem for mixed-convection flow past a horizontal plate

LJUBOMIR SAVIĆ AND HERBERT STEINRÜCK

Institute of Fluid Mechanics and Heat Transfer, Vienna University of Technology, Resselgasse 3, 1040 Vienna, Austria

(Received 19 June 2006 and in revised form 30 May 2007)

The flow near the trailing edge of a horizontal plate in a uniform parallel stream under a small angle of attack in the limit of large Reynolds number and large Grashof number is considered. Applying the concept of interacting boundary layers, a triple-deck problem taking the hydrostatic pressure perturbation into account can be formulated. However, it turns out that the interaction pressure is discontinuous at the trailing edge and thus new sublayers to resolve the discontinuity are introduced.

1. Introduction

The flow near the trailing edge of a horizontal heated plate which is aligned under a small angle of attack ϕ to the oncoming parallel flow with velocity U_∞ in the limit of large Reynolds $Re = U_\infty L/\nu$ and large Grashof $Gr = g\beta\Delta T L^3/\nu^2$ number will be investigated (figure 1). As usual β, ν and g denote the isobaric expansion coefficient, the kinematic viscosity and the acceleration due to gravity, respectively. The difference between the plate temperature and the temperature of the oncoming fluid is ΔT and L is the length of the plate. A measure for the influence of the buoyancy onto the boundary-layer flow along a horizontal plate is the buoyancy parameter $K = Gr\,Re^{-5/2}$ as defined in Schneider & Wasel (1985).

Mixed convection boundary-layer flows along an infinite horizontal surface have been investigated by several authors (Schneider 1979; Schneider & Wasel 1985; Merkin & Ingham 1987; Wickern 1991; Daniels 1992; Denier, Duck & Li 2005; Steinrück 1994; Lagree 1999). In contrast to the mixed convection flow along an inclined or vertical surface, where the buoyancy force has a component tangential to the main flow direction, in the case of the mixed convection flow over a horizontal surface buoyancy influences the boundary-layer flow only indirectly. The temperature difference across the boundary-layer induces a hydrostatic pressure distribution above the heated (or cooled) surface. Owing to the change of the temperature (density) profile along the surface, this hydrostatic pressure distribution has a non-vanishing component of its gradient tangential to the surface. Thus some authors (e.g. Gersten & Herwig 1992) speak of indirect free convection. However, it turns out that when the indirect buoyancy effect accelerates the flow, nothing unexpected happens regarding the solution of the boundary-layer equations. The modified boundary-layer equations can be integrated starting from the leading edge downstream. Near the leading edge, buoyancy effects play almost no role. Thus the velocity and temperature profiles are close to those of forced convection. Downstream, the indirect buoyancy effect accelerates the flow and very far downstream, the velocity and temperature profile tend to the similarity solution of the natural convection flow above a heated plate

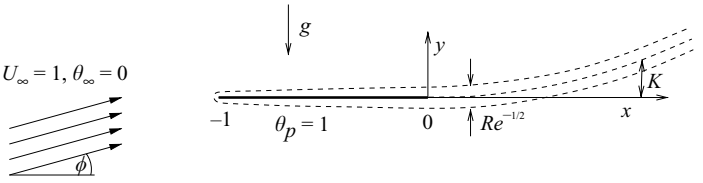

FIGURE 1. Mixed convection flow past a horizontal plate.

(cf. Schneider & Wasel 1985). This is the case of the flow above a heated plate or below the lower side of a cooled plate. A forward integration has been done by Steinrück (2001) and Lagree (2001). However, regarding stability, interesting phenomena occur which have been investigated by Denier, Stott & Bassom (2001).

In case of adverse buoyancy effects (flow above a cooled plate) it has been expected that the flow will decelerate and separation will occur. However, when trying to find out how the boundary-layer flow approaches the point of vanishing wall shear stress it turned out that the solution of the boundary-layer equations as a parabolic problem is not well posed. At least a one parametric family of solutions had been found (cf. Steinrück 1994). Thus it has been concluded that the solution of the boundary-layer equations might depend on the flow conditions at the trailing edge.

In order to avoid the numerical problems associated with forward integration of the boundary-layer equations, Denier *et al.* (2005) used a scheme which takes the downstream influences into account.

This downstream dependence of the mixed convection boundary-layer flow equations motivates us to study the behaviour of the flow near the trailing edge and the global flow field.

Schneider (2005) was the first to investigate the two-dimensional global flow field induced by mixed convection flow past a horizontal plate. He investigated the problem in the limit of a vanishing Prandtl number. For technical reasons he embedded the heated plate in a horizontal channel with a width proportional to $\ln Pe$ where Pe denotes the Péclet number. The main idea is that owing to the temperature perturbation in the wake, a hydrostatic pressure difference builds up across the wake which has to be compensated by a vortex sheet along the wake inducing a non-vanishing circulation and thus a lift force onto the plate.

We followed the ideas of Schneider (2005) in Savić & Steinrück (2005) where we studied the mixed convection flow around a finite plate for a small buoyancy parameter and a finite Prandtl number. Taking the inclination of the wake into account and assuming a small inclination, the technical assumption to place the plate in a horizontal channel could be avoided.

A second aspect of the flow around a finite plate is the analysis of the flow around the trailing edge. In the limit of large Reynolds number, triple-deck methods first introduced by Stewartson (1969) and Messiter (1970) have been applied to study the local flow behaviour at the trailing edge. The flow around a plate with a small angle of attack to the oncoming parallel flow has been investigated by Brown & Stewartson (1970) analytically and numerically by Chow & Melnik (1976).

In a first (unpublished) attempt we tried to follow the approach of Chow & Melnik (1976) and consider the mixed convection trailing-edge problem similar to the problem of a small angle of attack. However, it turned out that the present problem has some additional, perhaps even more complicating features, namely a discontinuity of the interaction pressure at the trailing edge on triple-deck scales. Thus additional sublayers will be introduced to resolve the pressure discontinuity.

The starting point of the analysis is the Navier–Stokes equations in dimensionless form for an incompressible fluid using the Bousinessq approximation to take buoyancy forces into account, the energy equation, and the continuity equation.

$$uu_x + vu_y = -p_x + \frac{1}{Re}(u_{xx} + u_{yy}), \tag{1.1a}$$

$$uv_x + vv_y = -p_y + \frac{1}{Re}(v_{xx} + v_{yy}) + \frac{Gr}{Re^2}\theta, \tag{1.1b}$$

$$u\theta_x + v\theta_y = \frac{1}{Re\,Pr}(\theta_{xx} + \theta_{yy}), \tag{1.1c}$$

$$u_x + v_y = 0. \tag{1.1d}$$

The flow is subjected to the asymptotic boundary conditions

$$u = 1, \quad v = \phi, \quad \theta = 0 \quad \text{for} \quad x^2 + y^2 \to \infty, \tag{1.2}$$

and the boundary conditions at the plate

$$u(x, 0) = v(x, 0) = 0, \quad \theta(x, 0) = 1, \quad -1 < x < 0. \tag{1.3}$$

In addition to the above mentioned dimensionless parameters, the Prandtl number $Pr = \nu/a$ where a is the thermal conductivity and the angle of attack ϕ enter the problem. The Prandtl number Pr is assumed to be of order 1.

The global structure of the flow field is shown in figure 1. The flow around the plate is a potential flow with the exception of the boundary layer at the plate and the wake where viscous effects play a role. Near the trailing edge of the plate the boundary layer interacts (locally) with the potential flow, and sublayers according to triple-deck theory (Stewartson 1969; Messiter 1970) will be introduced. To apply the triple-deck analysis it turns out that the buoyancy parameter K and the angle of attack ϕ have to be of the order $Re^{-1/4}$. Thus we define the reduced buoyancy parameter $\kappa = K\,Re^{1/4}$ and the reduced inclination parameter $\lambda = \phi K\sqrt{Re}$. We note that the choice of the magnitude of ϕ is not only dictated by the trailing-edge analysis, but it is a consequence of the analysis of the far field (see Savić & Steinrück 2005).

As we will see, the inclination parameter λ will play no role in the trailing-edge analysis. Only for positive values of λ does an outer potential flow field exist (cf. Savić & Steinrück 2005). We remark that in case of symmetric flow conditions (upper side of the plate heated, lower side cooled) the interaction mechanism would allow K to be larger, namely of order $Re^{-1/8}$. After a short review of the interaction of the wake with the potential flow (§ 2) the focus of the present paper will be the analysis of the flow near the trailing edge (§ 3). A numerical solution reveals that the interaction pressure is discontinuous at the trailing edge. Thus new sublayers are introduced to resolve the discontinuity (§ 4).

Before we start the analysis we will give some data for which the following theory applies. We must choose the Reynolds number Re to be, on one hand, sufficiently large that the asymptotic theory can be applied, but, on the other hand, to be below its critical value to ensure laminar flow. Thus Reynolds numbers in the range 10^4–10^5 are appropriate. The Grashof number Gr must be chosen such that the reduced buoyancy parameter is of order one. Thus the range of the Grashof number is from 10^8 to 10^{13}. Table 1 gives the data for air at room temperature.

In this paper we will use the following notation for the variables in different layers. Consider a sublayer of the dimensions $Re^{-\alpha/8}$ in the x- and $Re^{-\beta/8}$ in the y-direction. The corresponding independent variables are denoted by $x^{(\alpha)} = xRe^{\alpha/8}$ and $y^{(\beta)} = yRe^{\beta/8}$.

ν ($m^2\,s^{-1}$)	β (K^{-1})	ΔT (K)	U ($m\,s^{-1}$)	L (m)	Gr —	Re —	K —	κ —
1.513×10^{-5}	0.00334	6.87	0.1513	1	10^9	10^4	0.1	1
1.513×10^{-5}	0.00334	13.74	0.3026	2.5	3.125×10^{10}	10^5	0.00988	0.176

TABLE 1. Data for mixed convection flow for air at $p = 1$ bar, $T = 21.15\,^{\circ}$C.

The dependent variable u on that sublayer is denoted by

$$u^{(\alpha,\beta)}\big(x^{(\alpha)}, y^{(\beta)}\big) = u\big(x^{(\alpha)} Re^{-\alpha/8}, y^{(\beta)} Re^{-\beta/8}\big). \tag{1.4a}$$

For the pressure p and the temperature θ, an analogous notation will be used. The vertical velocity component v will be scaled such that the continuity equation written in the sublayer variables does not contain a scaling factor. Thus we define

$$v^{(\alpha,\beta)}\big(x^{(\alpha)}, y^{(\beta)}\big) = Re^{(\beta-\alpha)/8} v\big(x^{(\alpha)} Re^{-\alpha/8}, y^{(\beta)} Re^{-\beta/8}\big). \tag{1.4b}$$

Unless otherwise indicated, we use asymptotic expansions of the form

$$u(x, y) \sim u_0^{(\alpha,\beta)}\big(x^{(\alpha)}, y^{(\beta)}\big) + Re^{-1/8} u_1^{(\alpha,\beta)}\big(x^{(\alpha)}, y^{(\beta)}\big) + \cdots, \tag{1.5a}$$

for the horizontal velocity component u and analogous expansions for the pressure p, and temperature θ and on the (α, β) sublayer. For the vertical velocity component v we use expansions of the form

$$v(x, y) \sim Re^{(\beta-\alpha)/8}\big(v_0^{(\alpha,\beta)}\big(x^{(\alpha)}, y^{(\beta)}\big) + Re^{-1/8} v_1^{(\alpha,\beta)}\big(x^{(\alpha)}, y^{(\beta)}\big) + \cdots\big). \tag{1.5b}$$

on the (α, β) sublayer.

2. The global flow field

Before we begin the discussion of the global flow field we explain the chosen scaling of the buoyancy parameter $K = O(Gr/Re^{5/2})$. It is a measure for the hydrostatic pressure difference induced by the temperature perturbations across the boundary-layer or the wake, respectively. Thus this hydrostatic pressure difference across the wake must be compensated by the outer inviscid potential flow. On the other hand, the potential flow induces an inclination of the wake of order K. The component of the pressure gradient tangential to the centreline of the wake is given by the inclination of the wake, which is of order K times the vertical pressure gradient which is of order $K\sqrt{Re}$, since the thickness of the wake is of order $1/\sqrt{Re}$. Finally, we estimate the tangential component of the pressure gradient with $K^2\sqrt{Re}$ which must be order one to obtain a meaningful asymptotic limit. Thus we choose K and a possible inclination ϕ of the unperturbed parallel flow of order $Re^{-1/4}$.

In the following we give a brief summary of the analysis of the global flow field which is characterized by an interaction of the wake with the perturbation of the potential flow. For details, see Savić & Steinrück (2005).

2.1. *Boundary layer and wake*

The boundary-layer and wake are of thickness $Re^{-1/2}$. Since we have to expect an inclination of the wake, we introduce the stretched vertical coordinate as

$$y^{(4)} = \big(y - Re^{-1/4} y_w\big)\, Re^{1/2}, \tag{2.1}$$

where the centreline of the wake is given by $y = Re^{-1/4} y_w(x)$. In the boundary layer along the plate, $-1 < x < 0$, we set $y_w(x) = 0$. Perturbations of the pressure are expected to be of the order of the buoyancy parameter. Thus the pressure can be expanded in the form

$$p(x, y) \sim Re^{-1/4} p_2^{(\alpha,\beta)}\left(x^{(\alpha)}, y^{(\beta)}\right) + \cdots . \tag{2.2}$$

In the potential flow region we have $\alpha = \beta = 0$ and in the wake and boundary-layer $(\alpha, \beta) = (0, 4)$. Applying the usual scaling for the boundary-layer (and wake) we obtain for the leading-order terms the x-momentum, continuity and energy equation.

$$u_0^{(0,4)} \frac{\partial u_0^{(0,4)}}{\partial x^{(0)}} + v_0^{(0,4)} \frac{\partial u_0^{(0,4)}}{\partial y^{(4)}} = \kappa y_w' \theta_0^{(0,4)} + \frac{\partial^2 u_0^{(0,4)}}{\partial {y^{(4)}}^2}, \tag{2.3a}$$

$$\frac{\partial u_0^{(0,4)}}{\partial x^{(0)}} + \frac{\partial v_0^{(0,4)}}{\partial y^{(4)}} = 0, \tag{2.3b}$$

$$u_0^{(0,4)} \frac{\partial \theta_0^{(0,4)}}{\partial x^{(0)}} + v_0^{(0,4)} \frac{\partial \theta_0^{(0,4)}}{\partial y^{(4)}} = \frac{1}{Pr} \frac{\partial^2 \theta_0^{(0,4)}}{\partial {y^{(4)}}^2}. \tag{2.3c}$$

The y-momentum equation reduces to

$$\frac{\partial p_2^{(0,4)}}{\partial y^{(4)}} = \kappa \theta_0^{(0,4)}. \tag{2.3d}$$

Owing to the inclination of the wake, the hydrostatic pressure gradient has a non-vanishing component tangential to the wake. The inclination of the wake has to be determined from the potential flow. At the plate, $y_w' = 0$ holds and thus we have, to leading order, the Blasius solution for the boundary-layer flow,

$$u \sim u_B = f_B'\left(\frac{y^{(4)}}{\sqrt{x^{(0)} + 1}}\right), \quad \theta \sim \theta_B\left(\frac{y^{(4)}}{\sqrt{x^{(0)} + 1}}\right), \quad -1 < x < 0, \tag{2.4}$$

where f_B is the Blasius similarity solution and θ_B is the corresponding similarity solution for the temperature profile.

2.2. *Potential flow*

Integrating (2.3*d*) with respect to $y^{(4)}$ from $-\infty$ to ∞ we obtain

$$p_2^{(0,0)}(x, 0+) - p_2^{(0,0)}(x, 0-) = p_2^{(0,4)}(x, +\infty) - p_2^{(0,4)}(x, -\infty) = \kappa \gamma_w(x), \tag{2.5}$$

with

$$\gamma_w(x) = \int_{-\infty}^{\infty} \theta^{(0,4)}\left(y^{(4)}\right) \mathrm{d}y^{(4)}. \tag{2.6}$$

Equation (2.5) states that the temperature perturbation in the wake induces a hydrostatic pressure jump across the wake. Thus the potential flow has to satisfy the pressure jump condition (2.5), the tangential flow condition at the plate $v(x, 0) = 0$ for $-1 < x < 0$ and the asymptotic boundary condition (1.2).

Using the notation of complex functions we decompose the potential flow field as follows:

$$u - \mathrm{i}v = 1 - \mathrm{i}\phi \sqrt{\frac{z}{z+1}} + Re^{-1/4} \kappa \left(u_2^{(0,0)} - \mathrm{i}v_2^{(0,0)}\right) + \cdots, \tag{2.7}$$

with $z = x + \mathrm{i}y$. The first term corresponds to the potential flow around the plate under an angle of attack ϕ. The second part is due to a hydrostatic pressure difference

Symbol	Numerical value	Definition	Reference
a_0	0.3321	$a_0 = f_B''(0)$	
A_0	$0.8920\, a_0^{-1/3}$	$\bar{A}(x^{(3)}) \sim A_0 (x^{(3)})^{1/3},\ x^{(3)} \to \infty$	(3.8)
C_p	$0.6107\, a_0^{3/4}$	$\dfrac{\mathrm{d}\bar{p}_2^{(3,5)}}{\mathrm{d}x^{(3)}} \sim C_p (x^{(3)})^{-1/3},\ x^{(3)} \to 0+$	(3.43)
a_1	$1.343\, a_0$	$a_1 = \bar{u}_s'(0)$	Below (3.41)
a_2	$-0.301\, a_0^{7/4}$	$a_2 = \bar{u}_s''(0)$	Below (3.41)
c_1	$-1.644\, a_0^{-1}$	$E \sim c_1 \eta \ln \eta + c_2 \eta,\ \eta \to \infty$	(3.27)
c_2	$(0.724 - \dfrac{1.644}{3} \ln a_0) a_0^{-1}$		(3.27)
$[\Delta p]$	$5.27\, a_0^{-3/4}$	$[\Delta p] = -\Delta p^{(3,5)}(0-, 0)$	(3.35*c*)
$C_{u,\log}$	$-0.168 [\Delta p]\, a_0^{-1/4}$	$[\Delta u] = C_{u,\log} \ln y^{(5)} + C_{u,0},\ y^{(5)} \to 0$	(3.40)
$C_{u,0}$	$(0.042 - 0.168 \frac{3}{4} \ln a_0)[\Delta p] a_0^{-1/4}$		(3.41)

TABLE 2. Constants and their definition.

across the wake. Formally, the second part can be considered as being induced by a vortex distribution of strength $\kappa \gamma_w(x)$ along the plate and wake. Whereas in the wake, the vortex distribution γ_w is equal to the pressure jump across the wake, the vortex distribution γ_P at the plate has to be determined such that the tangential flow condition holds.

Using (2.7), the scaled inclination of the wake is given by

$$y_w'(x) = \frac{\lambda}{\kappa} \sqrt{\frac{x}{x+1}} + \kappa v_2^{(0,0)}(x, 0). \tag{2.8}$$

For $v_2^{(0,0)}$ an integral representation in terms of the vortex distribution γ_w in the wake can be derived. We have

$$v_2^{(0,0)}(x) = \frac{1}{2\pi} \sqrt{\frac{x}{x+1}} \int_0^\infty \frac{\gamma_w(\xi)}{x - \xi} \sqrt{\frac{\xi + 1}{\xi}}\, \mathrm{d}\xi, \tag{2.9}$$

(see Savić & Steinrück 2005). For non-vanishing values of κ, the flow in the wake and the potential flow correction due to buoyancy have to be solved simultaneously.

Here we summarize the most important results of the wake–potential flow interaction problem. A detailed analysis and discussion of the solution can be found in Savić & Steinrück (2005).

(i) Considering the far field of the wake flow, it turns out that solutions exist only for positive values of λ.

(ii) Solutions exist only for reduced buoyancy parameters κ less than a critical value $\kappa_c(\lambda)$ which depends on λ. For $\lambda = 1$, this critical value is about 0.914.

(iii) The local behaviour of the potential flow field near the trailing-edge is

$$u_2^{(0,0)}(x, 0+) \sim \begin{cases} -\dfrac{\gamma_{w,0}}{2} - \dfrac{\gamma_{w,1}}{2} \left| x^{1/3} \right|, & x > 0, \\ -\dfrac{\gamma_{w,0}}{2} - \gamma_{w,1} \left| x^{1/3} \right|, & x < 0, \end{cases} \tag{2.10}$$

$$v_2^{(0,0)}(x, 0) \sim -\frac{\sqrt{3}}{2} \gamma_{w,1} \left| x^{1/3} \right|, \quad x > 0, \tag{2.11}$$

with $\gamma_{w,0} = 2 \int_0^\infty \theta_B(y)\, \mathrm{d}y$, $\gamma_{w,1} = -2A_0$, with A_0 given in table 2.

3. Trailing edge

For the analysis of the flow field near the trailing edge the velocities, pressure and temperature are decomposed into a symmetric and antisymmetric part

$$\bar{u}(x,y)=\frac{u(x,y)+u(x,-y)}{2},\quad \Delta u=\frac{u(x,y)-u(x,-y)}{2Re^{-1/4}\kappa}. \tag{3.1}$$

All other dependent variables, with the exception of the vertical velocity component v, are decomposed accordingly. We decompose the vertical velocity v as

$$\bar{v}(x,y)=\frac{v(x,y)-v(x,-y)}{2},\quad \Delta v=\frac{v(x,y)+v(x,-y)}{2Re^{-1/4}\kappa}. \tag{3.2}$$

The definitions (1.4*a*), (1.4*b*) and the notation for the expansions (1.5*a*), (1.5*b*) are applied to the symmetric and antisymmetric parts of the flow, pressure and temperature fields accordingly. We rewrite the basic equation for mixed convection flow in terms of the symmetric and antisymmetric parts using the boundary-layer coordinates $x^{(0)}$, $y^{(4)}$

$$\bar{u}^{(0,4)}\frac{\partial\bar{u}^{(0,4)}}{\partial x^{(0)}}+\bar{v}^{(0,4)}\frac{\partial\bar{u}^{(0,4)}}{\partial y^{(4)}}+\frac{\kappa^2}{Re^{1/2}}\left(\Delta u^{(0,4)}\frac{\partial\Delta u^{(0,4)}}{\partial x^{(0)}}+\Delta v^{(0,4)}\frac{\partial\Delta u^{(0,4)}}{\partial y^{(4)}}\right)$$
$$=-\frac{\partial\bar{p}^{(0,4)}}{\partial x^{(0)}}+\frac{\partial^2\bar{u}^{(0,4)}}{\partial\left(y^{(4)}\right)^2}+\frac{1}{Re}\frac{\partial^2\bar{u}^{(0,4)}}{\partial\left(x^{(0)}\right)^2}, \tag{3.3}$$

$$\frac{1}{Re}\left(\bar{u}^{(0,4)}\frac{\partial\bar{v}^{(0,4)}}{\partial x^{(0)}}+\bar{v}^{(0,4)}\frac{\partial\bar{v}^{(0,4)}}{\partial y^{(4)}}\right)+\frac{\kappa^2}{Re^{3/2}}\left(\Delta u^{(0,4)}\frac{\partial\Delta v^{(0,4)}}{\partial x^{(0)}}+\Delta v^{(0,4)}\frac{\partial\Delta v^{(0,4)}}{\partial y^{(4)}}\right)$$
$$=-\frac{\partial\bar{p}^{(0,4)}}{\partial y^{(4)}}+\frac{\kappa^2}{Re^{1/2}}\Delta\theta^{(0,4)}+\frac{1}{Re}\frac{\partial^2\bar{v}^{(0,4)}}{\partial\left(y^{(4)}\right)^2}+\frac{1}{Re^2}\frac{\partial^2\bar{v}^{(0,4)}}{\partial\left(x^{(0)}\right)^2}. \tag{3.4}$$

Thus in the equations for the symmetric part, the reduced buoyancy parameter κ appears in the terms of order $Re^{-1/2}$. However, these terms do not influence the equations for leading-order terms of the triple-deck analysis. For the antisymmetric parts, we obtain

$$\bar{u}^{(0,4)}\frac{\partial\Delta u^{(0,4)}}{\partial x^{(0)}}+\Delta u^{(0,4)}\frac{\partial\bar{u}^{(0,4)}}{\partial x^{(0)}}+\bar{v}^{(0,4)}\frac{\partial\Delta u^{(0,4)}}{\partial y^{(4)}}+\Delta v^{(0,4)}\frac{\partial\bar{u}^{(0,4)}}{\partial y^{(4)}}$$
$$=-\frac{\partial\Delta p^{(0,4)}}{\partial x^{(0)}}+\frac{\partial^2\Delta u^{(0,4)}}{\partial\left(y^{(4)}\right)^2}+\frac{1}{Re}\frac{\partial^2\Delta u^{(0,4)}}{\partial\left(x^{(0)}\right)^2}, \tag{3.5}$$

$$\frac{1}{Re}\left(\bar{u}^{(0,4)}\frac{\partial\Delta v^{(0,4)}}{\partial x^{(0)}}+\Delta u^{(0,4)}\frac{\partial\bar{v}^{(0,4)}}{\partial x^{(0)}}+\bar{v}^{(0,4)}\frac{\partial\Delta v^{(0,4)}}{\partial y^{(4)}}+\Delta v^{(0,4)}\frac{\partial\bar{v}^{(0,4)}}{\partial y^{(4)}}\right)$$
$$=-\frac{\partial\Delta p^{(0,4)}}{\partial y^{(4)}}+\bar{\theta}^{(0,4)}+\frac{1}{Re}\frac{\partial^2\Delta\bar{v}^{(0,4)}}{\partial\left(y^{(4)}\right)^2}+\frac{1}{Re^2}\frac{\partial^2\Delta v^{(0,4)}}{\partial\left(x^{(0)}\right)^2}. \tag{3.6}$$

If the symmetric parts of the flow and pressure field are known, the equations for the antisymmetric parts are linear and independent of κ.

Thus for the leading-order terms of the symmetric part, the classical triple-deck problem (cf. Stewartson 1969; Messiter 1970) is obtained. For an asymptotic description, the upper deck (3,3)-region, main deck (3,4)-region and lower deck (3,5)-region have to be considered. Here we summarize the leading-order terms of the

asymptotic expansion of the symmetric part of the velocity and pressure field in the triple deck region:

$$\bar{u}(x,y) = \begin{cases} 1 + Re^{-1/4}\bar{u}_2^{(3,3)}\big(x^{(3)}, y^{(3)}\big) + \cdots, \\ u_B\big(y^{(4)}\big) + Re^{-1/8}\bar{A}(x^{(3)})u_B'\big(y^{(4)}\big) + \cdots, \\ Re^{-1/8}\bar{u}_1^{(3,5)}\big(x^{(3)}, y^{(5)}\big) + \cdots, \end{cases} \tag{3.7a}$$

$$\bar{v}(x,y) = \begin{cases} Re^{-1/4}\bar{v}_2^{(3,3)}\big(x^{(3)}, y^{(3)}\big) + \cdots, \\ -Re^{-1/4}\bar{A}'\big(x^{(3)}\big)u_B\big(y^{(4)}\big) + \cdots, \\ Re^{-3/8}\bar{v}_1^{(3,5)}\big(x^{(3)}, y^{(5)}\big) + \cdots, \end{cases} \tag{3.7b}$$

$$\bar{p}(x,y) \sim \begin{cases} Re^{-1/4}\bar{p}_2^{(3,3)}\big(x^{(3)}, y^{(3)}\big) + \cdots, \\ Re^{-1/4}\bar{p}_2^{(3,4)}\big(x^{(3)}\big) + \cdots, \\ Re^{-1/4}\bar{p}_2^{(3,5)}\big(x^{(3)}\big) + \cdots, \end{cases} \tag{3.7c}$$

with $\bar{p}_2^{(3,3)}(x^{(3)}, 0) = \bar{p}_2^{(3,4)}(x^{(3)}) = \bar{p}_2^{(3,5)}(x^{(3)})$.

According to Stewartson (1969), the function $\bar{A}$ can be interpreted as the negative displacement thickness. We recall that the asymptotic behaviour of the negative displacement thickness $\bar{A}$ is given by

$$\bar{A}\big(x^{(3)}\big) \sim A_0\big(x^{(3)}\big)^{1/3} \quad \text{as} \quad x^{(3)} \to \infty, \tag{3.8}$$

with the constant A_0 given in table 2. In analogy to the velocity profile of the symmetric part in the main deck, the temperature profile of the symmetric part is given as

$$\theta \sim \theta_B\big(y^{(4)}\big) + Re^{-1/8}\bar{A}\big(x^{(3)}\big)\theta_B'\big(y^{(4)}\big). \tag{3.9}$$

In the following, we will discuss the interaction problem for the antisymmetric part of the solution.

3.1. *The* (3,4)*-region: main deck*

We start with the main deck $(\alpha, \beta) = (3, 4)$, then using the upper deck (3,3)-layer we derive the interaction law and finally derive the lower deck (3,5)-layer problem. The antisymmetric part of the pressure in the main deck can be expanded in the form

$$\Delta p = \Delta p_0^{(3,4)} + Re^{-1/8}\Delta p_1^{(3,4)} + \cdots. \tag{3.10}$$

In contrast to (classical) triple-deck problems, the pressure is not constant across the main deck. The pressure involved in the interaction mechanism is of order $Re^{-1/8}$, i.e. $\Delta p_1^{(3,4)}$. The y-momentum equation reduces to

$$\frac{\partial \Delta p_0^{(3,4)}}{\partial y^{(4)}} = \bar{\theta}_0^{(3,4)}, \quad \frac{\partial \Delta p_1^{(3,4)}}{\partial y^{(4)}} = \bar{\theta}_1^{(3,4)}, \tag{3.11}$$

with $\bar{\theta}_0^{(3,4)} = \theta_B$ and $\bar{\theta}_1^{(3,4)} = \bar{A}\theta_B'$. Using (3.9), we obtain

$$\Delta p_0^{(3,4)}\big(x^{(3)}, y^{(4)}\big) = \int_\infty^{y^{(4)}} \theta_B\big(\tilde{y}^{(4)}\big)\,\mathrm{d}\tilde{y}^{(4)} + \Delta p_0^{(0,0)}(0,0), \tag{3.12a}$$

$$\Delta p_1^{(3,4)}\big(x^{(3)}, y^{(4)}\big) = \bar{A}\big(x^{(3)}\big)\theta_B\big(y^{(4)}\big) + \Delta p_1^{(3,3)}(x_3, 0). \tag{3.12b}$$

Note that according to (2.2) and (3.1) we have $\Delta p_0^{(0,0)} = (1/\kappa)p_2^{(0,0)}$.

The expansions for the velocity components Δu and Δv follow the same lines as Stewartson (1969) and the solution of the equations of the leading-order terms can be expressed in terms of an as yet undetermined function ΔA of $x^{(3)}$, which can be interpreted as the scaled difference of the negative displacement thicknesses on the upper and lower side of the plate. The leading-order terms of the antisymmetric part of the velocity components are given as

$$\Delta u = \ln Re \frac{c_1}{f_B''(0)} f_B''\big(y^{(4)}\big) + \Delta A\big(x^{(3)}\big) f_B''\big(y^{(4)}\big) + C_1\big(y^{(4)}\big) + \cdots, \tag{3.13a}$$

$$\Delta v = -Re^{-1/8} \Delta A'\big(x^{(3)}\big) f_B'\big(y^{(4)}\big) + \cdots. \tag{3.13b}$$

The term of the magnitude $\ln Re$ and the term $C_1(y^{(4)})$ are both independent of $x^{(3)}$ and arise from matching the main deck solution, (3,4)-region, with the solution of the boundary-layer equations, (0,4)-region, for the antisymmetric part of the flow field, cf. (3.32). The constant c_1 will be defined later in (3.27). In table 2, all constants, their numerical values and their definitions are summarized.

3.2. *The* (3,3)*-region: upper deck*

Since the flow in the upper deck is a potential flow with the velocity field

$$\Delta u - \mathrm{i}\Delta v = \Delta u_0^{(0,0)}(0,0) + Re^{-1/8}\big(\Delta u_1^{(3,3)}\big(x^{(3)}, y^{(3)}\big) - \mathrm{i}\Delta v_1^{(3,3)}\big(x^{(3)}, y^{(3)}\big)\big) + \cdots, \tag{3.14}$$

where $\Delta u_0^{(0,0)}(0,0) = (1/\kappa)u_2(0,0+)$, see (2.7), and $\Delta u_1^{(3,3)}(x^{(3)},0) = -\Delta p_1^{(3,3)}(x^{(3)},0)$, $\Delta v_1^{(3,3)}(x^{(3)},0) = -\Delta A'(x^{(3)})$ holds, the pressure $\Delta p_1^{(3,3)}(x^{(3)},0)$ and the negative displacement thickness $\Delta A(x^{(3)})$ can be interpreted as the real and imaginary parts of a complex analytical function $\Delta\Phi_1$ evaluated on the real axis. We have

$$\begin{aligned}\Delta\Phi_1\big(x^{(3)},0\big) &= -\Delta p_1^{(3,3)}\big(x^{(3)},0\big) + \mathrm{i}\Delta A'\big(x^{(3)}\big)\\ &= -\big(\Delta p_1^{(3,4)}\big(x^{(3)},0\big) - \bar{A}\big(x^{(3)}\big)\big) + \mathrm{i}\Delta A'\big(x^{(3)}\big).\end{aligned} \tag{3.15}$$

Considering $\Delta p_1^{(3,4)}(x^{(3)},0) = 0$ for $x^{(3)} > 0$ and using the asymptotic behaviour of $\bar{A}$ for $x^{(3)} \to \infty$, we conclude that

$$\Delta\Phi_1(z) \sim (a + \mathrm{i}b) z^{1/3} \quad \text{for} \quad z \to \infty \tag{3.16}$$

holds. The constants a and b are determined by using $\Delta A' \to 0$ for $x^{(3)} \to -\infty$. They turn out to be $a = A_0$ and $b = -\sqrt{3}A_0$. Thus the asymptotic behaviour of $\Delta p_1^{(3,5)}$ and $\Delta A'$ is given by

$$\Delta p_1^{(3,4)}\big(x^{(3)},0\big) \sim -2A_0\big|x^{(3)}\big|^{1/3} \quad \text{for} \quad x^{(3)} \to -\infty, \tag{3.17}$$

$$\Delta A'\big(x^{(3)}\big) \sim -\sqrt{3}A_0\big|x^{(3)}\big|^{1/3} \quad \text{for} \quad x^{(3)} \to \infty. \tag{3.18}$$

Note that if $\Delta p_1^{(3,5)} - \bar{A}(x^{(3)})$ tends to different constants for $x^{(3)} \to \infty$ and $x^{(3)} \to -\infty$, the real part of the complex function $\Delta\Phi_1 - (a+\mathrm{i}b)z^{1/3}$ would tend to different constant values for $x^{(3)} \to -\infty$ and $x^{(3)} \to \infty$. Thus the next-order term in the expansion of Φ_1 for $z \to \infty$ would be of the form $\mathrm{i}\ln z$, contradicting the requirement that $\Delta A'$ vanishes for $x^{(3)} \to -\infty$. Thus a possible constant in the expansion of $\Delta p_1^{(3,4)}$ for $x^{(3)} \to -\infty$ must be the same constant as in the expansion of $\Delta p_1^{(3,4)} - \bar{A}$ for $x^{(3)} \to \infty$. However, using the fact that $\Delta p_1^{(3,4)}(x^{(3)}) = 0$ for $x^{(3)} > 0$ and equation (4.4*a*) in Stewartson (1969) we conclude that this constant must vanish, thus showing that $\Delta\Phi_1(z) - (a + \mathrm{i}b)z^{1/3} \to 0$ as $z \to \infty$.

Finally, the interaction law can be written in the form

$$\Delta A'\big(x^{(3)}\big) + \sqrt{3}A_0 h\big(x^{(3)}\big)\big(x^{(3)}\big)^{1/3} = -\left[\frac{1}{\pi}\int_{-\infty}^{0} \frac{\Delta p_1^{(3,4)}(\xi,0) + 2A_0|\xi|^{1/3}}{x^{(3)}-\xi}\,\mathrm{d}\xi - \frac{1}{\pi}\int_{-\infty}^{\infty} \frac{\bar{A}(\xi) - A_0 h(\xi)|\xi|^{1/3}}{x^{(3)}-\xi}\,\mathrm{d}\xi\right], \quad (3.19)$$

where $h(x)$ denotes the Heaviside function with $h(x)=1$ for $x>0$ and $h(x)=0$ for $x<0$.

We have written the interaction law in such a form that the singular parts are separated and the integrand in the Hilbert integral decays sufficiently fast to zero for $x^{(3)} \to \pm\infty$.

The asymptotic behaviour of the vertical velocity component v for $x^{(3)} \to \infty$ and $y^{(4)} \to \pm\infty$ is given by

$$\begin{aligned} v &= \pm\bar{v} + \kappa Re^{-1/4}\Delta v \\ &\sim -\big(\kappa Re^{-3/8}\Delta A' f_B'\big(y^{(4)}\big) \pm Re^{-2/8}\bar{A}' f_B'\big(y^{(4)}\big)\big) \\ &= \kappa Re^{-3/8}\sqrt{3}A_0\big(x^{(3)}\big)^{1/3} f_B'\big(y^{(4)}\big) \pm Re^{-2/8}\tfrac{1}{3}A_0\big(x^{(3)}\big)^{-2/3} f_B'\big(y^{(4)}\big) \\ &= \kappa Re^{-2/8}\sqrt{3}A_0\big(x^{(0)}\big)^{1/3} \pm Re^{-4/8}\tfrac{1}{3}A_0\big(x^{(0)}\big)^{-2/3}. \end{aligned} \quad (3.20)$$

Thus the vertical component v in the main deck matches with its counterpart in the potential flow region (2.7), (2.11).

3.3. *The lower deck*

The equations for the velocity profile in the lower deck are given by the momentum equation in the x-direction,

$$\bar{u}_1^{(3,5)}\frac{\partial\Delta u_0^{(3,5)}}{\partial x^{(3)}} + \Delta u_0^{(3,5)}\frac{\partial\bar{u}_1^{(3,5)}}{\partial x^{(3)}} + \bar{v}_1^{(3,5)}\frac{\partial\Delta u_0^{(3,5)}}{\partial y^{(5)}} + \Delta v_0^{(3,5)}\frac{\partial\bar{u}_1^{(3,5)}}{\partial y^{(5)}} = -\frac{\partial\Delta p_1^{(3,5)}}{\partial x^{(3)}} + \frac{\partial^2\Delta u_0^{(3,5)}}{\big(\partial y^{(5)}\big)^2}, \quad (3.21)$$

the continuity equation, and the momentum equation in the y-direction which reduces to

$$0 = -\frac{\partial\Delta p_1^{(3,5)}}{\partial y^{(5)}} + \bar{\theta}_B(0). \quad (3.22)$$

The boundary conditions are

$$\Delta u_0^{(3,5)}\big(x^{(3)},0\big) = \Delta v_0^{(3,5)}\big(x^{(3)},0\big) = 0, \quad x^{(3)}<0 \quad \text{for the plate,} \quad (3.23a)$$

$$\Delta u_0^{(3,5)}\big(x^{(3)},0\big) = \Delta p_1^{(3,5)}\big(x^{(3)},0\big) = 0, \quad x^{(3)}>0 \quad \text{for the wake.} \quad (3.23b)$$

We remark that changes of the temperature profile in the lower deck are too small to influence the leading-order terms of the hydrostatic pressure distribution and thus a discussion of the energy equation is not necessary.

Integrating (3.22), we obtain the pressure difference in the lower deck

$$p_1^{(3,5)}\big(x^{(3)},y^{(5)}\big) = \theta_B(0)y^{(5)} + p_1^{(3,5)}\big(x^{(3)},0\big), \quad (3.24)$$

which matches with the pressure difference in the main deck (3.12). Thus $\Delta p_1^{(3,4)}(x^{(3)},0) = \Delta p_1^{(3,5)}(x^{(3)},0)$ and in the interaction law, (3.19), $\Delta p_1^{(3,4)}$ can be replaced by $\Delta p_1^{(3,5)}$.

It remains to specify the asymptotic behaviour of the velocity profile for $x^{(3)} \to -\infty$ and $y^{(5)} \to \infty$.

Considering the asymptotic behaviour of the pressure $\Delta p_1^{(3,5)}$ and of $\bar{u}_1^{(3,5)} \sim f_B''(0) y^{(5)}$ for $x^{(3)} \to -\infty$, we conclude that the asymptotic behaviour of the flow field $\Delta u_0^{(3,5)}$, $\Delta v_0^{(3,5)}$ in the lower deck is self-similar. Using a scaled streamfunction E defined by

$$\Delta u_0^{(3,5)} \sim E'(\eta) \quad \text{with} \quad \eta = \frac{y^{(5)}}{\left|x^{(3)}\right|^{1/3}}, \tag{3.25}$$

we obtain the similarity equation for E

$$3E''' - f_B''(0)\left(\eta^2 E'' - \eta E' + E\right) = 2A_0, \tag{3.26}$$

with the boundary conditions $E(0) = E'(0) = 0$.

The corresponding homogeneous equation has three linearly independent solutions $e_1(\eta) \sim \eta \ln \eta$ for $\eta \to \infty$, $e_2(\eta) = \eta$ and $e_3(\eta)$. The third solution, e_3, increases at least exponentially for $\eta \to \infty$. In order to match the velocity profile with the solution of the main deck problem e_3 has to be eliminated. Thus, we have

$$E(\eta) = -\frac{2A_0}{f_B''(0)} + c_1 e_1(\eta) + c_2 e_2(\eta) \sim -\frac{2A_0}{f_B''(0)} + c_1 \eta \ln \eta + c_2 \eta, \quad \eta \to \infty. \tag{3.27}$$

Since there are two boundary conditions at $\eta = 0$, the constants c_1 and c_2 are uniquely defined. Their values can be found in table 2. The corresponding velocity profile is shown in figure 4 labelled with $x^{(3)} = -\infty$. The asymptotic behaviour of the velocity profile for $x^{(3)} \to -\infty$, $y^{(5)} \to \infty$ is given by

$$\Delta u_0\left(x^{(3)}, y^{(5)}\right) \sim E'(\eta) \sim c_1 \ln y^{(5)} - \frac{c_1}{3} \ln \left|x^{(3)}\right| + c_1 + c_2. \tag{3.28}$$

To supplement the lower deck equation (3.21) with the correct asymptotic boundary condition for $y^{(5)} \to \infty$, we need a condition which is satisfied by the derivatives with respect to $y^{(5)}$ of all linear combinations of the two admissible fundamental solutions 1 and $\ln y^{(5)}$ of the linear ordinary differential equation (3.26). Such a condition is given by

$$y^{(5)} \frac{\partial^2 \Delta u_0^{(3,5)}}{\partial \left(y^{(5)}\right)^2} + \frac{\partial \Delta u_0^{(3,5)}}{\partial y^{(5)}} \to 0 \quad \text{for} \quad y^{(5)} \to \infty. \tag{3.29}$$

The negative displacement thickness ΔA is given by

$$\Delta A\left(x^{(3)}\right) = \lim_{y^{(5)} \to \infty} \left(\Delta u_0^{(3,5)} - y^{(5)} \ln y^{(5)} \frac{\partial \Delta u_0^{(3,5)}}{\partial y^{(5)}} \right). \tag{3.30}$$

The $y^{(5)}$ independent part of the asymptotic behaviour of $u_0^{(3,5)}$ can be interpreted as the asymptotic behaviour of the negative displacement thickness ΔA. Thus, we have

$$\Delta A\left(x^{(3)}\right) \sim (c_1 + c_2) - \frac{c_1}{3} \ln \left|x^{(3)}\right| \quad \text{as} \quad x^{(3)} \to -\infty. \tag{3.31}$$

Expanding the boundary layer for the antisymmetric part of the flow field near the trailing edge $0 < -x^{(0)} \ll 1$, the flow field has a viscous sublayer and an inviscid main part. The solution of the viscous sublayer is again given by the similarity solution E. Matching the sublayer with the main part introduces a logarithmic term in the

inviscid main part. We have:

$$\Delta u^{(0,4)} = \begin{cases} E'\left(\dfrac{y^{(4)}}{\left|x^{(0)}\right|^{1/3}}\right) & \text{for} \quad \left(y^{(4)}\right)^3 \sim \left|x^{(0)}\right|, \\ C_1\left(y^{(4)}\right) - \dfrac{c_1}{3f_B''(0)} \ln\left|x^{(0)}\right| f_B''\left(y^{(4)}\right) + \cdots & \text{for} \quad (y^{(4)})^3 \gg \left|x^{(0)}\right|, \end{cases} \tag{3.32}$$

with the asymptotic behaviour of C_1 given by $C_1(y^{(4)}) \sim c_1 \ln y^{(4)}$ for $y^{(4)} \to 0$.

Matching the inviscid main part of the boundary layer (3.32) yields the anticipated expansion of the main deck (3.13*b*).

3.4. *Numerical solution*

The lower deck equations with the interaction law for the antisymmetric part of the flow field are solved using Veldman's iteration method (cf. Veldmann & van de Vooren 1975). For a better comparison with the numerical results in the existing literature, the lower deck problem has been rescaled by the following transform:

$$\left.\begin{array}{llll} & x^{(3)} = a_0^{-5/4} X, & y^{(5)} = a_0^{-3/4} Y, & \\ \bar{u}_1^{(3,5)} = a_0^{1/4} \bar{U}, & \bar{v}_1^{(3,5)} = a_0^{3/4} \bar{V}, & \bar{p}_1^{(3,5)} = a_0^{1/2} \bar{P}, & \bar{A} = a_0^{-3/4} \bar{\mathscr{A}}, \\ \Delta u_0^{(3,5)} = a_0^{-1} \Delta U, & \Delta v_0^{(3,5)} = a_0^{-1/2} \Delta V, & \Delta p_1^{(3,5)} = a_0^{-3/4} \Delta P, & \Delta A = a_0^{-2} \Delta \mathscr{A}, \end{array}\right\} \tag{3.33}$$

with $a_0 = f_B''(0) = 0.3321$ (cf. (3.1.42) in Sychev *et al.* 1998). Using the transform (3.33), the lower deck equations for the symmetric and antisymmetric part stay invariant with the exception of the matching condition of $\bar{u}^{(3,5)} \to a_0 y^{(5)}$ for $x^{(3)} \to -\infty$ or $y \to \infty$ which transforms into $\bar{U} \to Y$ for $X \to -\infty$ or $Y \to \infty$. In the following, we use the transformed variables as far as the numerical method is concerned. The solution itself will be discussed in the original variables.

In the x-direction, a stretched grid has been used with $X_{i+1} - X_i = f(X_i - X_{i-1})$ for $1 < i < N$, and $X_{-i} = -X_i$. The minimal step size is $X_1 - X_0 = 0.001$ with $X_0 = 0$, the factor f is $f = 1.01$ and the number of intervals $2N$ with $N = 400$. Thus the computational domain is $(-10^7, 10^7)$. In order to capture the asymptotic behaviour for $x^{(3)} \to -\infty$ correctly, the 'similarity' variable

$$\tilde{\eta} = a_0^{1/3} \frac{y^{(5)}}{\left(\sqrt{\left(x^{(3)}\right)^2 + a_0^{-5/2}}\right)^{1/3}} = \frac{Y}{(\sqrt{X^2+1})^{1/3}} \tag{3.34}$$

is used instead of $y^{(5)}$ as the second independent variable. For the numerical solution, the asymptotic boundary condition (3.29) has been posed at $\tilde{\eta} = 20$.

At X_{-N}, the similarity solution for the velocity profile is described. The momentum equation (3.21) is discretized with backward differences with respect to X. At each node X_i, an ordinary differential equation for the velocity profile at X_i and the value of the difference of the negative displacement thicknesses $\Delta A(x_i)$ as additional unknown is obtained. The system of ordinary differential equations is solved on the interval (0, 20) for the 'similarity' variable $\tilde{\eta}$ using the ODE solver COLPAR, which uses a B-spline collocation method (cf. Ascher, Christiansen & Russel 1981).

It turned out that the Veldman iteration method converges only very slowly, especially near the discontinuity of the pressure $\Delta p_1^{(3,5)}$ at $x^{(3)} = 0$. About 10 000 iterations have been performed to obtain the pressure $\Delta p_1^{(3,5)}(0-, 0)$ with an accuracy of 10^{-2}.

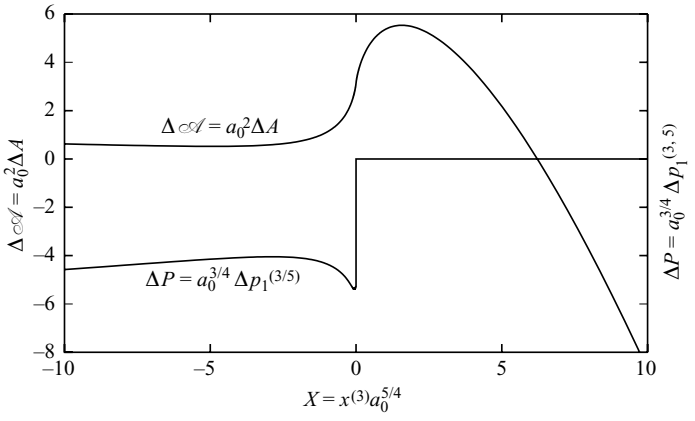

FIGURE 2. Negative displacement thickness ΔA and interaction pressure $\Delta p_1^{(3,5)}(x^{(3)}, 0)$.

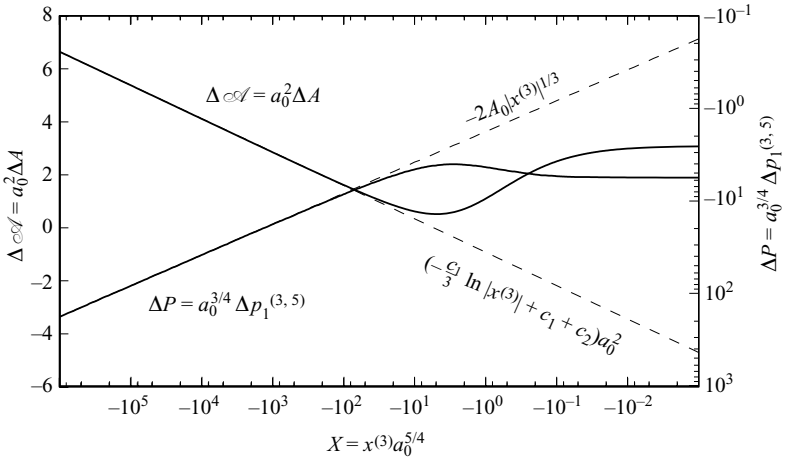

FIGURE 3. Asymptotic behaviour of ΔA, and $\Delta p_1^{(3,5)}(x^{(3)}, 0)$ for $x^{(3)} \to -\infty$.

Since $\Delta p_1^{(3,5)}(x^{(3)}, 0) = 0$ for $x^{(3)} > 0$, it is sufficient to solve the lower deck equations (3.21) and (3.29) together with the matching condition (3.30) and the interaction law (3.19) for $x^{(3)} \leqslant 0$ only. After convergence for ΔA is obtained, the velocity profile $\Delta u_0^{(3,5)}$ for $x^{(3)} > 0$ can be determined.

In figure 2, the negative displacement thickness ΔA and the interaction pressure $\Delta p_1^{(3,5)}(x^{(3)}, 0)$ for the antisymmetric part of the flow field are shown.

The asymptotic behaviour for $x^{(3)} \to -\infty$ of ΔA and $\Delta p_1^{(3,5)}$ is shown in figure 3 on a logarithmic and double logarithmic scale, respectively.

The term $-\Delta A'$ can be considered as the inclination of the near wake. Thus at the trailing edge, the wake first bends downwards and then turns upwards. For $x^{(3)} \to \infty$, we have $-\Delta A' \sim \sqrt{3}A_0(x^{(3)})^{1/3}$ which matches with $y'_w = v_2^{(0,0)}(x, 0)$ for $x \to 0$, see (2.11).

3.5. *The local behaviour of the lower deck velocity field near the trailing edge*

The interaction pressure $p_1^{(3,5)}$ has a jump discontinuity at the trailing edge $x^{(3)} = 0$. As a consequence, the derivative of the displacement thickness $\Delta A'$ has a logarithmic singularity at $x = 0$. To discuss the behaviour of the velocity profile $\Delta u^{(3,5)}$, we

integrate the momentum equation (3.21) across the jump discontinuity at $x^{(3)}=0$. We use the fact that the symmetric part of the flow field $\bar{u}_0^{(3,5)}$, $\bar{v}_0^{(3,5)}$ is continuous. Let

$$[\Delta u]\big(y^{(5)}\big) = \Delta u_0^{(3,5)}\big(0+, y^{(5)}\big) - \Delta u_0^{(3,5)}\big(0-, y^{(5)}\big), \tag{3.35a}$$

$$[\Delta p] = \Delta p_1^{(3,5)}(0+) - \Delta p_1^{(3,5)}(0-), \tag{3.35b}$$

$$V\big(y^{(5)}\big) = \lim_{\epsilon\to 0}\int_{-\epsilon}^{\epsilon} \Delta v_0^{(3,5)}\big(x^{(3)}, y^{(5)}\big)\,\mathrm{d}x^{(3)}, \tag{3.35c}$$

denote the jump in the Δu-component, the jump in the interaction pressure $\Delta p_1^{(3,5)}$ and the integral of the Δv-component across the jump discontinuity, respectively. Integrating the momentum equation (3.21) across the discontinuity at $x^{(3)}=0$, we obtain the ordinary differential equation for V

$$\bar{u}_s V' - V\bar{u}_s' = [\Delta p], \tag{3.36}$$

with the general solution

$$V\big(y^{(5)}\big) = [\Delta p]\int_{\infty}^{y^{(5)}} \frac{\bar{u}_s\big(y^{(5)}\big)}{(\bar{u}_s(\zeta))^2}\mathrm{d}\zeta + B\bar{u}_s\big(y^{(5)}\big), \tag{3.37}$$

where B is a constant and $\bar{u}_s(y^{(5)})=\bar{u}_1^{(3,5)}(0, y^{(5)})$. The jump in Δu_0 is therefore given by

$$[\Delta u]\big(y^{(5)}\big) = -V' = -[\Delta p]\frac{1}{\bar{u}_s\big(y^{(5)}\big)} - \left([\Delta p]\int_{\infty}^{y^{(5)}} \frac{\mathrm{d}\zeta}{(\bar{u}_s(\zeta))^2} + B\right)\bar{u}_s'\big(y^{(5)}\big). \tag{3.38}$$

Since the displacement thickness ΔA is continuous, we conclude that $[\Delta u]\to 0$ as $y^{(5)}\to\infty$ and thus $B=0$. Considering the behaviour of $[\Delta u]$ for $y^{(5)}\to 0$, we obtain

$$[\Delta u] \sim C_{u,\log}\ln y^{(5)} + C_{u,0} \tag{3.39}$$

with

$$C_{u,\log} = [\Delta p]\frac{a_2}{a_1^2}, \tag{3.40}$$

$$C_{u,0} = [\Delta p]\left(\frac{a_2}{a_1^2}\ln a_1 - a_1\int_{\infty}^{0}\ln u_s\left(\frac{\bar{u}_s''}{(\bar{u}_s')^3}\right)'\mathrm{d}\zeta\right), \tag{3.41}$$

with $a_1=\bar{u}_s'(0)$, and $a_2=\bar{u}_s''(0)=(\mathrm{d}\bar{p}_2^{(3,5)}/\mathrm{d}x^{(3)})(0-)$. Their numerical values can be found in Sychev *et al.* (1998) or in Chow & Melnik (1976) and are listed together with the numerical values of $C_{u,\log}$ and $C_{u,0}$ in table 2. In order to satisfy the boundary condition $\Delta u_0^{(3,5)}(x,0)=0$, a sublayer has to be introduced.

3.6. *A viscous sublayer*

According to Stewartson (1969), the symmetric part of the velocity field in the lower deck also has a sublayer as $x^{(3)}\to 0+$ owing to the abrupt change of the boundary conditions at $x^{(3)}=0$. The horizontal velocity component has the expansion

$$\bar{u}_1^{(3,5)} \sim \big(x^{(3)}\big)^{1/3}F'(\xi) + \bar{u}_s\big(y^{(5)}\big) - a_1 y^{(5)}, \qquad 0 < x^{(3)} \ll 1, \tag{3.42}$$

with $\xi = y^{(5)}/(x^{(3)})^{1/3}$, where F is the solution of the boundary-value problem

$$F''' + \tfrac{2}{3}F\,F'' - \tfrac{1}{3}(F')^2 = C_P, \quad F(0)=F'(0)=0, \quad F''(\infty)=a_1, \tag{3.43}$$

and the constant $C_P = 0.6107$ (see Chow & Melnik 1976) is given by the local behaviour of the interaction pressure $\partial\bar{p}_2^{(3,5)}/\partial x^{(3)} \sim C_P\,(x^{(3)})^{-1/3}$ for $0<x\ll 1$.

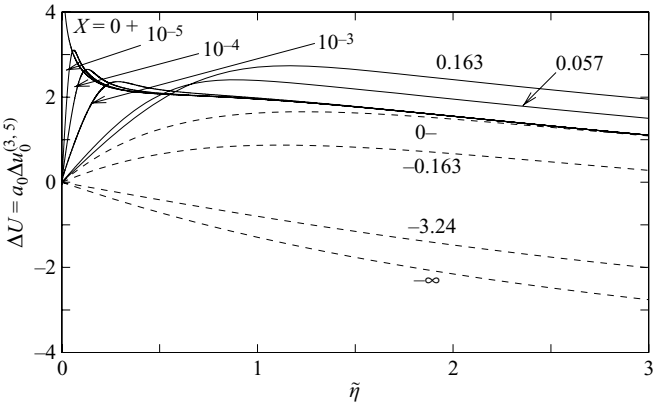

FIGURE 4. Velocity profiles $\Delta u^{(3,5)}$ at different locations $x^{(3)} = a_0^{-5/4} X$.

In order to compensate the logarithmic behaviour of $[\Delta u]$ we make the following ansatz for the velocity difference:

$$\Delta u_0^{(3,5)} \sim \Delta u_0^{(3,5)}\big(0-, y^{(5)}\big) + [\Delta u]\big(y^{(5)}\big) + \ln x^{(3)} G'(\xi) + H'(\xi) - C_{u,\log} \ln y - C_{u,0}, \quad \text{for} \quad 0 < x^{(3)} \ll 1, \tag{3.44}$$

where the functions G and H satisfy the similarity equations

$$\tfrac{1}{3}\left(F'G' - 2F\,G'' - F''G\right) = G''', \quad G'(0) = 0, \tag{3.45}$$

$$\tfrac{1}{3}\left(F'H' - 2F\,H'' - F''H\right) + F'G' - F''G = H''', \quad H'(0) = 0. \tag{3.46}$$

Asymptotic boundary conditions for G and H will be deduced from matching with the outer expansion of $\Delta u_0^{(3,5)}$; but before proceeding, we discuss the limiting behaviour for F, G and H. According to Stewartson (1969), $F \sim a_1 \xi^2/2$ for $\xi \to \infty$. Thus for $\xi \gg 1$, (3.45) and (3.46) reduce to

$$\frac{a_1}{3}\left(\xi G' - \xi^2 G'' - G\right) = G'', \tag{3.47}$$

$$\frac{a_1}{3}(\xi H' - \xi^2 H'' - H + \xi G' - G) = H''. \tag{3.48}$$

Thus (3.45) has three linearly independent solutions G_1, G_2 and G_3 and with $G_1 \sim \xi$, $G_2 \sim \xi \ln \xi$ and $G_3 \to 0$ for $\xi \to \infty$. Thus we obtain the following asymptotic boundary conditions for G and H

$$G \sim \frac{C_{u,\log}}{3}\xi, \quad H \sim C_{u,\log}\xi \ln \xi + (C_{u,0} - C_{u,\log})\xi, \quad \xi \to \infty. \tag{3.49}$$

The numerical solutions of the similarity equations (3.45) and (3.46) are shown in figure 5. Their asymptotic behaviour given by (3.49) is also indicated.

Now the velocity profile $\Delta u_0^{(3,5)}$ for $x^{(3)} > 0$ can be determined. As boundary condition at the discontinuity, we prescribe the local asymptotic expansion (3.44) at $X = 10^{-3}$. In figure 4 the velocity profiles for different values of X are shown. The velocity profiles at $X = 0+$, 10^{-5}, 10^{-4} and 10^{-3} are obtained by evaluating the local asymptotic expansion (3.44). The other profiles are obtained by numerical integration of the momentum equation (3.21).

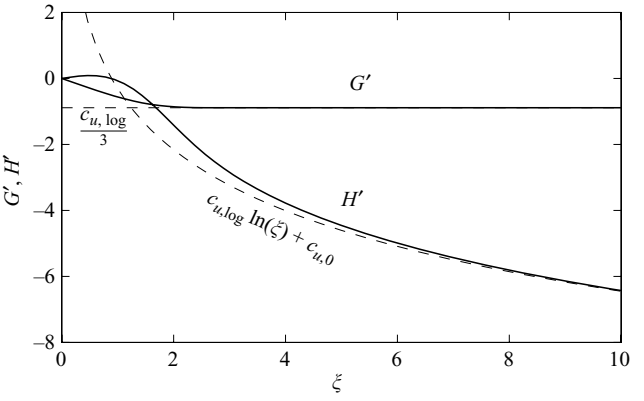

FIGURE 5. Similarity functions for velocity profiles in the viscous sublayer and their asymptotic behaviour (3.49) (dashed lines).

4. Additional sublayers

In order to resolve the discontinuity of the interaction pressure, additional sublayers will be introduced. An overview with the extensions of the sublayers in the x- and y-direction is given in figure 7.

4.1. *The* (4,4)*-region*

Because of the discontinuity of the difference pressure $\Delta p_1^{(3,5)}$ in the lower deck at the trailing edge, the pressure difference has a discontinuity in the main deck as well. In the upper deck, the pressure difference $\Delta p_1^{(3,3)}$ is singular at $(0,0)$. Using the calculus of analytic functions of a complex variable $z^{(3)} = x^{(3)} + \mathrm{i}y^{(3)}$ we can infer the behaviour of $\Delta p_1^{(3,3)}$ close to 0. The velocity field in the upper deck is given locally by

$$\Delta u_1^{(3,3)} - \mathrm{i}\Delta v_1^{(3,3)} \sim \bar{A}(0) - \frac{[\Delta p]}{\pi}\mathrm{i}\,\ln z = \bar{A}(0) + \frac{[\Delta p]}{\pi}\left(\arctan\frac{y}{x} - \mathrm{i}\ln\sqrt{x^2+y^2}\right). \tag{4.1}$$

Thus the pressure and the derivative of the displacement thickness behave locally as

$$\Delta p_1^{(3,3)} \sim -\bar{A}(0) - \frac{[\Delta p]}{\pi}\arctan\frac{y^{(3)}}{x^{(3)}}, \quad \Delta A'\big(x^{(3)}\big) \sim -\frac{[\Delta p]}{\pi}\ln\big|x^{(3)}\big|. \tag{4.2}$$

In order to resolve the discontinuity in the main deck we introduce the (4,4)-sublayer. The velocity profile has to match with the (3,4)-region (3.13*b*), (3.13*b*). Thus we use the following expansion of the antisymmetric part

$$\Delta u \sim \ln Re\frac{c_1}{f_B''(0)}f_B''\big(y^{(4)}\big) + \Delta u_0^{(3,4)}\big(0, y^{(4)}\big) + Re^{-1/8}\ln Re\frac{[\Delta p]}{8\pi}x^{(4)}f_B''\big(y^{(4)}\big) + Re^{-1/8}\Delta u_1^{(4,4)}\big(x^{(4)}, y^{(4)}\big) + \cdots, \tag{4.3a}$$

$$\Delta v \sim -Re^{-1/8}\ln Re\frac{[\Delta p]}{8\pi}f_B'\big(y^{(4)}\big) + Re^{-1/8}v_1^{(4,4)}\big(x^{(4)}, y^{(4)}\big) + \cdots, \tag{4.3b}$$

$$\Delta p \sim \Delta p_0^{(0,4)}\big(0, y^{(4)}\big) + Re^{-1/8}\Delta p_1^{(4,4)}\big(x^{(4)}, y^{(4)}\big) + \cdots. \tag{4.3c}$$

The term of order $Re^{-1/8}\ln Re$ in the vertical velocity component Δv arises from matching with the main deck solution and the logarithmic behaviour of $\Delta A'$ as $x^{(3)} \to 0$. As a consequence, a term of the same magnitude must be present in the expansion of the horizontal velocity component Δu. However, in the expansion of

the pressure Δp these 'logarithmic' terms are missing. The constant c_1 has been introduced in (3.27).

We obtain the following equations for the leading-order terms

$$f_B' \frac{\partial \Delta u_1^{(4,4)}}{\partial x^{(4)}} + \Delta v_1^{(4,4)} f_B'' = -\frac{\partial \Delta p_1^{(4,4)}}{\partial x^{(4)}}, \tag{4.4a}$$

$$f_B' \frac{\partial \Delta v_1^{(4,4)}}{\partial x^{(4)}} = -\frac{\partial \Delta p_1^{(4,4)}}{\partial y^{(4)}} + \bar{\theta}_1^{(0,4)}, \tag{4.4b}$$

$$\frac{\partial \Delta u_1^{(4,4)}}{\partial x^{(4)}} + \frac{\partial \Delta v_1^{(4,4)}}{\partial y^{(4)}} = 0. \tag{4.4c}$$

The flow in the (4,4)-sublayer is inviscid; but in contrast to the main deck, the y-momentum equation is not degenerate. Eliminating $\Delta u_1^{(4,4)}$ and $\Delta v_1^{(4,4)}$, an elliptic equation for $\Delta p_1^{(4,4)}$ can be derived,

$$f_B' \left[\frac{\partial^2 \Delta p_1^{(4,4)}}{\partial \left(x^{(4)}\right)^2} + \frac{\partial^2 \Delta p_1^{(4,4)}}{\partial \left(y^{(4)}\right)^2} - \frac{\partial \bar{\theta}_1^{(0,4)}}{\partial y^{(4)}} \right] + 2 f_B'' \left[\bar{\theta}_1^{(0,4)} - \frac{\partial \Delta p_1^{(4,4)}}{\partial y^{(4)}} \right] = 0. \tag{4.5}$$

The boundary and matching conditions can be expressed as

$$\Delta p_1^{(4,4)} \sim -\frac{|\Delta p|}{\pi} \arctan \frac{y^{(4)}}{x^{(4)}} + \bar{A}(0)\left(\theta_B\left(y^{(4)}\right) - 1\right), \tag{4.6}$$

for $y^{(4)} = 0$ or $r^{(4)} = \sqrt{(x^{(4)})^2 + (y^{(4)})^2} \to \infty$. We note that (4.6) represents the solution of the Laplace equation. Equation (4.5) becomes the Laplace equation if f_B'' is zero, which is the case for $y^{(4)} \to \infty$. The matching condition (4.6) for $r^{(4)} \to \infty$ is obtained from matching $\Delta p_1^{(4,4)}$ with the upper deck solution (4.2) and the main deck solution. The boundary condition at $y^{(4)} = 0$, $x^{(4)} < 0$ follows from (4.4*a*) and $v_1^{(4,4)}(x^{(4)}, 0) = 0$ for $x^{(4)} < 0$ which in turn is a consequence that ΔA and thus $\Delta u_0^{(3,4)}$ is continuous at $x^{(3)} = 0$.

For the numerical solution, we decompose the solution of the linear elliptic partial differential equation (4.5) into a particular solution and a solution of the homogenous problem:

$$\Delta p_1^{(4,4)} = -\frac{|\Delta p|}{\pi} \Delta p_h^{(4,4)}\left(y^{(4)}, x^{(4)}\right) + \bar{A}(0)\left(\theta_B\left(y^{(4)}\right) - 1\right), \tag{4.7}$$

with $\Delta p_h^{(4,4)} \sim \arctan y^{(4)}/x^{(4)}$ for $(x^{(4)})^2 + (y^{(4)})^2 \to \infty$ and $\Delta p_h^{(4,4)}(x^{(4)}, 0) = \pi$ for $x < 0$ and $\Delta p_h(x^{(4)}, 0) = 0$ for $x > 0$.

The local behaviour near the singularity can be discussed by transforming (4.5) to polar coordinates $r^{(4)}, \varphi$. Expanding $\Delta p_h^{(4,4)} \sim \Delta p_{h,0}(\varphi) + O(r^{(4)})$ for $r^{(4)} \ll 1$ we obtain

$$\sin\varphi \, \Delta p_{h,0}'' - 2\cos\varphi \Delta p_{h,0} = 0, \quad \Delta p_{h,0}(0) = 0, \quad \Delta p_{h,0}(\pi) = \pi, \tag{4.8}$$

with the solution

$$\Delta p_{h,0} = \varphi - \tfrac{1}{2}\sin 2\varphi. \tag{4.9}$$

A numerical solution for Δp_h is shown in figure 6. The correct asymptotic behaviour for $r^{(4)} \to 0$ and $r^{(4)} \to \infty$ could be verified.

4.2. *The* (4,5)*-region*

Since, in the (4,4)-region, the viscosity has been neglected, a sublayer with respect to the vertical coordinate y is necessary. Inspecting the momentum equation in the

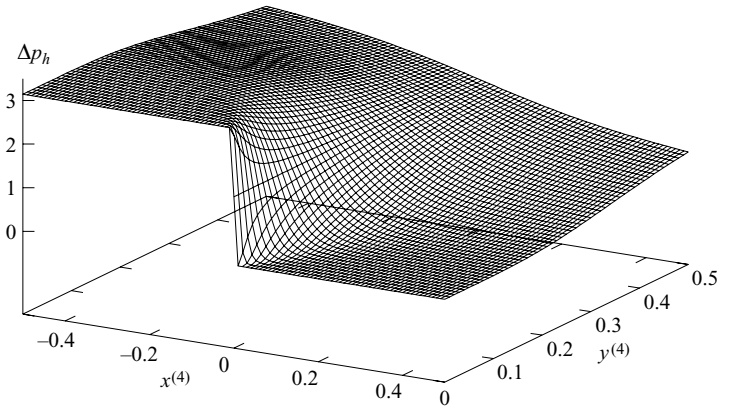

FIGURE 6. Local behaviour of the interaction pressure $\Delta p_1^{(4,4)}$ near the trailing edge. The solution Δp_h of the homogenous problem, cf. (4.7), is shown.

x-direction it turns out that the thickness of this layer is of the order of $Re^{-2/3}$. In our notation this would be a $(4, 5\frac{1}{3})$-layer, since $\frac{2}{3} = \frac{16}{3}\frac{1}{8}$. For convenience of notation we will denote this layer (4,+) and the corresponding vertical variable $y^{(+)}$.

In order to match the velocities in the (4,+)-region to those in the (3,5)-region and the (4,4)-region, the intermediate (4,5)-scale has to be introduced. The velocity and pressure field in that region are given by

$$\Delta u^{(4,5)} \sim \Delta u_0^{(3,5)}\big(0-, y^{(5)}\big) + h\big(x^{(3)}\big)[\Delta u]\big(y^{(5)}\big) + \cdots, \tag{4.10a}$$

$$\Delta v \sim Re^{-1/8}\Delta v^{(4,5)} \sim Re^{-1/8}\Delta v_1^{(4,4)}\big(x^{(3)}, 0\big) + \cdots, \tag{4.10b}$$

$$\Delta p \sim \Delta p_0^{(0,0)} - \int_0^\infty \theta_B\big(y^{(4)}\big)\mathrm{d}y^{(4)} + Re^{-1/8}h\big(-x^{(4)}\big)[\Delta p] + \cdots, \tag{4.10c}$$

where $h(x)$ is the Heaviside function.

4.3. *The* $(4, 5\frac{1}{3})$*-region*

Since the velocity profile in the (4,5)-region does not satisfy the boundary condition $\Delta u = 0$ at $y = 0$, it is necessary to introduce an additional sublayer. Since the pressure is constant there, we can find a similarity solution for the velocity field,

$$\Delta u \sim -\tfrac{1}{8}\ln Re\, G'(\xi^+) + \ln x^{(4)} G'(\xi^+) + H'(\xi^+), \tag{4.11a}$$

$$\begin{aligned}\Delta v \sim{}& \frac{1}{24}Re^{-1/6}\ln Re\,\big(x^{(4)}\big)^{-2/3}(G - \xi^+ G') \\ &+ Re^{-1/6}\big(x^{(4)}\big)^{-2/3}\left(-\frac{1}{3}\ln x^{(4)}(G - \xi^+ G') - \left(G + \frac{1}{3}H - \frac{\xi^+}{3}H'\right)\right),\end{aligned} \tag{4.11b}$$

where G and H are the same similarity functions as in (3.44) and $\xi^+ = y^{(+)}/(x^{(4)})^{1/3}$.

4.4. *The* (5,5)*-region*

In the (5,5) sublayer of the lower deck, a similar analysis as in the (4,4)-region applies. We use the expansion

$$\Delta u \sim \Delta u_0^{(5,5)}\big(x^{(5)}, y^{(5)}\big), \quad \Delta v \sim \Delta v_0^{(5,5)}\big(x^{(5)}, y^{(5)}\big), \tag{4.12a}$$

$$\Delta p \sim \Delta p_0^{(0,4)}(0, 0) + Re^{-1/8}\Delta p_1^{(5,5)}(x^{(5)}, y^{(5)}), \tag{4.12b}$$

and obtain the equations for the leading-order terms

$$\bar{u}_s \frac{\partial \Delta u_0^{(5,5)}}{\partial x^{(5)}} + \Delta v_0^{(5,5)} \bar{u}_s' = -\frac{\partial \Delta p_1^{(5,5)}}{\partial x^{(5)}}, \tag{4.13a}$$

$$\bar{u}_s \frac{\partial \Delta v_0^{(5,5)}}{\partial x^{(5)}} = -\frac{\partial \Delta p_1^{(5,5)}}{\partial y^{(5)}} + \theta_B(0), \tag{4.13b}$$

$$\frac{\partial \Delta u_0^{(5,5)}}{\partial x^{(5)}} + \frac{\partial \Delta v_0^{(5,5)}}{\partial y^{(5)}} = 0, \tag{4.13c}$$

where $\bar{u}_s(y^{(5)}) = \bar{u}_1^{(3,5)}(0, y^{(5)})$ denotes the velocity profile of the lower deck solution of the symmetric part at the trailing edge. Integrating (4.13*a*)–(4.13*c*) with respect to $x^{(5)}$ over $(-\infty, \infty)$ and defining

$$V\left(y^{(5)}\right) = \int_{-\infty}^{\infty} \Delta v_0^{(5,5)}\left(x^{(5)}, y^{(5)}\right) \mathrm{d}x^{(5)}, \tag{4.14}$$

the ordinary differential equation (3.36) for V can be re-derived. Manipulating (4.13*a*)–(4.13*c*), an elliptic differential equation for $\Delta p_1^{(5,5)}$ can be deduced,

$$\bar{u}_s \left(\frac{\partial^2 \Delta p_1^{(5,5)}}{\partial \left(x^{(5)}\right)^2} + \frac{\partial^2 \Delta p_1^{(5,5)}}{\partial \left(y^{(5)}\right)^2} \right) - 2\bar{u}_s' \left(\frac{\partial \Delta p_1^{(5,5)}}{\partial y^{(5)}} - \theta_B(0) \right) = 0, \tag{4.15}$$

with the matching and boundary conditions

$$\Delta p_1^{(5,5)} = -\frac{[\Delta p]}{\pi}\left(\varphi - \tfrac{1}{2}\sin 2\varphi\right) + \theta_B(0) y^{(5)}, \tag{4.16}$$

where $\varphi = \arctan y^{(5)}/x^{(5)}$ for $r^{(5)} \to \infty$, $\varphi = 0$ and $\varphi = \pi$, respectively. Moreover, (4.16) also describes the local behaviour for $r^{(5)} \to 0$ since $\bar{u}_s/\bar{u}_s' \to 1$ for both $y^{(5)} \to \infty$ and $y^{(5)} \to 0$.

The pressure $\Delta p_1^{(5,5)}$ is everywhere continuous except at the trailing edge $x^{(5)} = 0$, $y^{(5)} = 0$. Thus we have resolved the pressure discontinuity to a single point on triple-deck scales.

If the pressure field $\Delta p_1^{(5,5)}$ is known, we can determine the velocities in the (5,5)-layer. We insert the continuity equation (4.13*c*) into (4.13*a*) and obtain the first-order differential equation for $\Delta v_0^{(5,5)}$,

$$-\bar{u}_s \frac{\partial \Delta v_0^{(5,5)}}{\partial y^{(5)}} + \Delta v_0^{(5,5)} \bar{u}_s' = -\frac{\partial \Delta p_1^{(5,5)}}{\partial x^{(5)}}. \tag{4.17}$$

Integration of (4.17) and matching with the (4,4)-region yields

$$\Delta v_0^{(5,5)} = \bar{u}_s\left(y^{(5)}\right) \int_{\infty}^{y^{(5)}} \frac{1}{\bar{u}_s^2} \frac{\partial \Delta p_1^{(5,5)}}{\partial x^{(5)}} \,\mathrm{d}\tilde{y}^{(5)}. \tag{4.18}$$

Using that $\bar{u}_s(0) = 0$ and $\partial \Delta p_1^{(5,5)}/\partial x^{(5)} = 0$ for $x^{(5)} < 0$, we conclude that $\Delta v^{(5,5)}(x^{(5,0)}) = 0$ for $x^{(5)} < 0$. Using (4.13*c*), we obtain

$$\begin{aligned} \Delta u_0^{(5,5)} = -u_s'\left(y^{(5)}\right) \int_{\infty}^{y^{(5)}} \frac{1}{\bar{u}_s^2} \left(\Delta p_1^{(5,5)}\left(x^{(3)}, \tilde{y}^{(5)}\right) - \Delta p_1^{(3,5)}\left(0-, \tilde{y}^{(5)}\right)\right) \mathrm{d}\tilde{y}^{(5)} \\ - \frac{1}{\bar{u}_s}\left(\Delta p_1^{(5,5)}\left(x^{(3)}, y^{(5)}\right) - \Delta p_1^{(3,5)}\left(0-, y^{(5)}\right)\right) + \Delta u_0^{(3,5)}\left(0-, y^{(5)}\right). \end{aligned} \tag{4.19}$$

The asymptotic behaviour of $\Delta u^{(5,5)}$ for $y^{(5)} \to 0$ is given by

$$\Delta u_0^{(5,5)} \sim \begin{cases} \tilde{C}_{u,0}\left(x^{(5)}\right), & x^{(5)} < 0, \\ C_{u,\log} \ln y^{(5)} + \tilde{C}_{u,0}\left(x^{(5)}\right), & x^{(5)} > 0, \end{cases} \tag{4.20}$$

where $C_{u,\log}$ is defined in (3.40), $\tilde{C}_{u,0}(-\infty) = 0$ and $\tilde{C}_{u,0}(\infty) = C_{u,0}$.

4.5. *The* $(5, 5\frac{2}{3})$*-region*

In order to satisfy the boundary condition $\Delta u = 0$ at $y = 0$, a sublayer has to be introduced. The appropriate scaling factor for the vertical coordinate turns out to be $Re^{17/24}$. Thus we define the stretched vertical coordinate $y^{(*)} = Re^{17/24} y = Re^{1/12} y^{(5)}$. Note in the notation (1.4*a*), (1.4*b*) we would have to write $y^{(17/3)}$. Instead of the superscript (17/3) we write the superscript (*).

Matching with the (5,5)-region requires an asymptotic expansion of the horizontal velocity component of the form

$$\Delta u^{(5,*)} \sim \begin{cases} -\frac{1}{4} \ln Re\, G'(\xi^*) + \Delta u_0^{(5,*)}\left(x^{(5)}, y^{(*)}\right) + \cdots, & x > 0, \\ \Delta u_0^{(5,*)}\left(x^{(5)}, y^{(*)}\right) + \cdots, & x < 0, \end{cases} \tag{4.21a}$$

$$\Delta v = Re^{-1/12} \Delta v^{(5,*)} \sim \begin{cases} \Delta v_0^{(5,5)}\left(x^{(5)}, 0\right) + Re^{-1/12} \left(\dfrac{\left(x^{(5)}\right)^{-2/3}}{12} (G - \xi^* G') \ln Re + \Delta v_0^{(5,*)} \right), & x > 0, \\ Re^{-1/12} \Delta v_0^{(5,*)} + \cdots, & x < 0, \end{cases} \tag{4.21b}$$

with $\xi^* = y^{(*)}/(x^{(5)})^{1/3}$ and the function G is the solution of the similarity equation (3.45) and the asymptotic boundary condition (3.49). The velocity field $\Delta u_0^{(5,*)}$, $\Delta v_0^{(5,*)}$ satisfies the linearized boundary-layer equation

$$\bar{u}_{1.5}^{(5,*)} \frac{\partial \Delta u_0^{(5,*)}}{\partial x^{(5)}} + \Delta u_0^{(5,*)} \frac{\partial \bar{u}_{1.5}^{(5,*)}}{\partial x^{(5)}} + \bar{v}_{1.5}^{(5,*)} \frac{\partial \Delta u_0^{(5,*)}}{\partial y^{(*)}} + \Delta v_0^{(5,*)} \frac{\partial \bar{u}_{1.5}^{(5,*)}}{\partial y^{(*)}} = \frac{\partial^2 \Delta u_0^{(5,*)}}{\left(\partial y^{(*)}\right)^2} \tag{4.22}$$

and the continuity equation with

$$\bar{u} \sim Re^{-3/16} \bar{u}_{1.5}^{(5,*)} + \cdots, \quad \bar{u}_{1.5}^{(5,*)} = \begin{cases} a_1 y^{(*)}, & x < 0, \\ \left(x^{(5)}\right)^{1/3} F'(\xi^*), & x > 0, \end{cases} \tag{4.23}$$

where the function F is the solution of (3.42).

The index 1.5 of $\bar{u}$ reflects the fact that the expansion of the symmetric part of the velocity field in this layer is of the order $(Re^{1/8})^{1.5} = Re^{3/16}$.

For a complete resolution of the discontinuity, an analysis of the (6,6)-region where the complete Navier–Stokes equations are the governing equations for the leading-order terms would be necessary.

5. Summary and conclusions

An analysis of the mixed convection flow around a finite horizontal plate under a small angle of attack in the limit of large Reynolds number and small buoyancy effects has been performed. Surprising results have been obtained regarding the flow

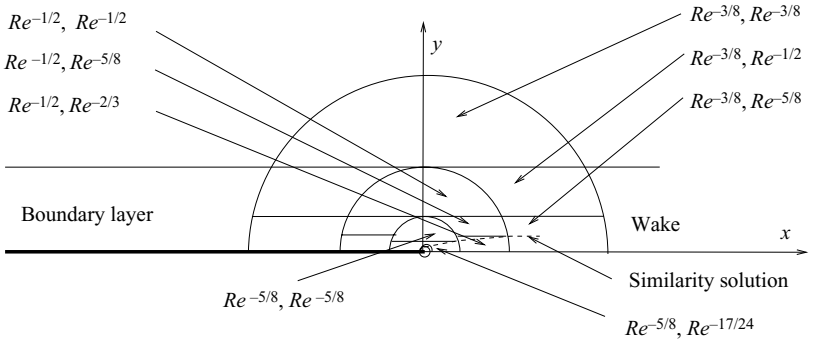

FIGURE 7. The sublayers and their thickness in the x- and y-direction near the trailing edge. The dotted line represents the domain where the velocity profile is represented by the similarity solution $\ln x^{(3)}G'(\xi) + H'(\xi)$, (3.44).

on the global scales and regarding the local analysis of the flow near the trailing edge as well. The main results are as follows.

(i) Solutions of the global flow problem exist only if the reduced buoyancy parameter κ is smaller than a critical value which depends on the reduced inclination parameter λ.

(ii) The local analysis of the mixed convection flow near the trailing edge revealed that the usual triple deck-structure of the flow near the trailing edge is not sufficient to describe the local flow behaviour. It turned out that the interaction pressure and the velocity profile in the lower deck are discontinuous at the trailing edge on triple-deck scales.

(iii) In order to resolve these discontinuities, new sublayers have been introduced and discussed. A schematic overview of the sublayers is given in figure 7.

(iv) However, a pressure singularity at the trailing edge remains even on the (5,5)-sublayer which can probably be resolved only on scales where the full Navier–Stokes equations apply.

(v) Although on triple-deck scales there is a pressure jump at the trailing edge on the scales of the potential flow (leading order) the pressure is continuous at the trailing edge satisfying the Kutta condition.

(vi) In the case of the flow of a fluid with a positive expansion coefficient past a heated plate, the fluid flows at the trailing edge first downwards then the wake turns, as expected, upwards.

For an experimental verification of the presented analysis for the global flow, one has to place the plate in a channel with lateral walls to prevent a flow around the lateral edges of the plate and the vortex sheet in the wake. We expect that two-dimensional local theory will be a good approximation of the flow field near the trailing edge sufficiently far away from the lateral edges.

The theory presented here can be carried over to the case when the hydrostatic pressure gradient is induced by the concentration of a resolved substance in the fluid instead of the temperature perturbations. In that case, the large Grashof number which is necessary to have a meaningful influence of buoyancy can be obtained more easily.

Though the local flow properties at the trailing-edge of the mixed convection flow past a horizontal plate are clarified, there are still open questions concerning the global flow field. For example what does the three-dimensional mixed convection flow

around a finite plate look like? What type of singularity occurs when approaching the critical value of the buoyancy parameter and what happens beyond the critical value? This will be the subject of further investigations.

The research was supported by the FWF Austrian Science fund, Project P14957. The authors thank Professor W. Schneider for many stimulating discussions.

REFERENCES

Ascher, U., Christiansen, J. & Russel, R. D. 1981 Collaction software for boundary value odes. *ACM Trans. Math. Software* **7**, 209–222.

Brown, S. N. & Stewartson, K. 1970 Trailing-edge stall. *J. Fluid Mech.* **42**, 561–584.

Chow, R. & Melnik, E. 1976 Numerical solutions of triple-deck equations for laminar trailing edge stall. *Tech. Rep.* RE-526J. Grumman Research Dept.

Daniels, P. G. 1992 A singularity in thermal boundary layer flow on a horizontal surface. *J. Fluid Mech.* **242**, 419–440.

Denier, J. P., Stott, J. A. K. & Bassom, A. P. 2001 Three dimensional inviscid waves in buoyant boundary-layer flows. *Fluid Dyn. Res.* **28**, 89–109.

Denier, J. P., Duck, P. W. & Li, J. 2005 On the growth (and suppression) of very short-scale disturbances in mixed forced–free convection boundary layers. *J. Fluid Mech.* **526**, 147–170.

Gersten, K. & Herwig, H. 1992 *Strömunsgmechanik*. Vieweg.

Lagree, P.-Y. 1999 Thermal mixed convection induced locally by a step change in surface temperature in a Poiseuille flow in the framework of triple deck theory. *Intl J. Heat Mass Transfer* **42**, 2509–2524.

Lagree, P.-Y. 2001 Removing the marching breakdown of boundary layer equations for mixed convection above a horizontal plate. *Intl J. Heat Mass Transfer* **44**, 3359–3372.

Merkin, J. H. & Ingham, D. B. 1987 Mixed convection similarity solutions on a horizontal surface. *Z. Angew. Math. Phys.* **38**, 102–116.

Messiter, A. F. 1970 Boundary layer flow near the trailing edge of flat plate. *SIAM J. Appl. Maths* **18**, 241–257.

Savić, Lj. & Steinrück, H. 2005 Mixed convection flow past a horizontal plate. *Theor. Appl. Mech.* **32**, 1–19.

Schneider, W. 1979 A similarity solution for combined forced and free convection flow over a horizontal plate. *Intl J. Heat Mass Transfer* **22**, 1401–1406.

Schneider, W. 2005 Lift, thrust and heat transfer due to mixed convection flow past a horizontal plate. *J. Fluid Mech.* **529**, 51–69.

Schneider, W. & Wasel, M. G. 1985 Breakdown of the boundary-layer approximation for mixed convection above a horizontal plate. *Intl J. Heat Mass Transfer* **28**, 2307–2313.

Steinrück, H. 1994 Mixed convection over a cooled horizontal plate: non-uniqueness and numerical instabilities of the boundary-layer equations. *J. Fluid Mech.* **278**, 251–265.

Steinrück, H. 2001 A review of the mixed convection boundary-layer flow over a horizontal cooled plate. *GAMM Mitteilungen* **24**, 127–158.

Stewartson, K. 1969 On the flow near the trailing edge of a flat plate. *Mathematica* **16**, 106–121.

Sychev, V. V., Ruban, A. I., Sychev, Vic. V. & Korolev, G. L. 1998 *Asymptoty Theory of Separated Flows*. Cambridge University Press.

Veldmann, A. E. P. & van de Vooren, A. I. 1975 *Drag of a Finite Plate*. Lecture Notes in Physics vol. 35. Springer.

Wickern, G. 1991 Mixed convection from an arbitrarily inclined semi-infinite plate. Part I. The influence of the inclination angle. *Intl J. Heat Mass Transfer* **34**, 1935–1945.